

# DAMAGE ACCUMULATION AND LIFETIME PREDICTION OF WOVEN GFRP UNDER CONSTANT TENSILE LOAD TEST IN HYDROCHLORIC ACID SOLUTION

M. Kotani<sup>1\*</sup>, Y. Yamamoto<sup>2</sup>, Y. Sato<sup>2</sup>, R. Sato<sup>2</sup> and H. Kawada<sup>1</sup>

<sup>1</sup> Department of Applied Mechanics and Aerospace Engineering, Waseda University, Tokyo, Japan,

<sup>2</sup> Department of Mechanics and Engineering, Graduate School of Waseda University, Tokyo, Japan

\* Corresponding author ([robot\\_5ta2@toki.waseda.jp](mailto:robot_5ta2@toki.waseda.jp))

**Keywords:** *GFRP, Delayed Fracture, Durability, Hydrochloric Acid, Water Environment, SCC*

## ABSTRACT

Constant tensile load tests of woven glass fiber reinforced plastics were conducted in air, in deionized water and in hydrochloric acid at 40°C. The delayed fracture occurred in both solutions but did not occur in air in the range of this research. The fracture time decreased with the increase in the applied stress and was shorter in hydrochloric acid than in deionized water. The resin adhesion on the glass fiber surface decreased with the increasing test time and the fracture surface of the glass fiber flattened with the decrease of the applied stress. These transitions in the fracture surfaces exhibit the strength degradation of the glass fiber and the fiber/matrix interfacial adhesion, i.e. the constituents of GFRP. The fracture time of the woven GFRP was predicted based on the assumption of the global load sharing (GLS).

## 1 Introduction

Glass-fiber reinforced plastics (GFRP) have superior corrosive resistance compared to metal materials and has various applications such as wind turbine, industrial facility, marine structural materials. In fact, GFRP operating in such services are based on damage tolerance design with excessive safety factor due to the lack of long-term reliability data. Unfortunately, some failure accidents of GFRP after long-term operation under corrosive environments are reported [1]. Thus, significant research has been carried out dealing with the strength degradation and crack propagation properties of GFRP in corrosive environment to evaluate its long-term durability. It was clarified through these researches that such accidents occur due to the degradation of the materials properties and the stress corrosion cracking (SCC) due to the interaction between the applied stress and the environmental agents [2]-[3].

In addition, it was clarified that the applied stress progresses the degradations and the increasing temperature accelerates such degradations intensely [4]-[5]. However, there are a few research which deals with the creep behavior of GFRP in corrosive environment. Jones has conducted a stress corrosion tests (creep test in H<sub>2</sub>SO<sub>4</sub>) of unidirectional GFRP and informed the transition of the fracture surface and reported the possibility of the threshold stress of fracture [6]. Kotani has conducted constant tensile load test of woven GFRP in hydrothermal environment and proposed the lifetime prediction method based on the energy criterion [7]. The predicted results showed good agreement by considering the degradation of the GFRP induced by hydrothermal aging and its acceleration with increasing temperature. In fact, there are GFRP constituents that possess high corrosion resistance and the failure mechanism of corrosion resistant GFRP in corrosive environment is still uncertain. It is therefore required to clarify the mechanism of the delayed fracture and to propose the lifetime prediction method.

There are significant researches proposing the prediction method on lifetime and mechanical properties of composite materials. Turon has reported the possibility to calculate the mechanical properties of unidirectional composite by considering the degradation within its constituents from Weibull parameters obtained from the fiber fragmentation test [8]. Kotani has predicted the strength degradation of unidirectional GFRP after hydrothermal aging based on the assumption of global load sharing (GLS) and considering the strength degradation of the glass fiber and the fiber/matrix interfacial adhesion [9]. The predicted results showed good agreement with the experimental data while considering the strength

degradations of the glass fiber and the fiber/matrix interfacial adhesion which are obtained from the fiber fragmentation test.

Present paper discusses the fracture mechanism of corrosion resistant GFRP, consisted with NCR-glass fiber and vinylester resin, in air, in deionized water and in hydrochloric acid. Firstly, static tensile load tests of woven GFRP were conducted in each environment in order to evaluate its mechanical properties. Constant tensile load tests were conducted in air, in deionized water and in hydrochloric acid to measure the fracture time and the strain history. Finally, the fracture time of the constant tensile load test was predicted using the strength of the constituents, i.e. glass fiber, matrix resin and fiber/matrix interfacial adhesion.

## 2 Experimental

### 2.1 Specimen

The specimen under study is the woven GFRP consisted by plain NCR-glass cloth for the fiber reinforcement and vinylester resin for the matrix which both possess high corrosion resistance. The material properties of the constituents are summarized in Table 1. The GFRP plates were fabricated by hot-press molding. The GFRP specimens were cut from the plate, and the edges of each specimen were polished using emery paper in order to avoid edge effects. The specimen geometry for the static tensile tests and the constant tensile load tests was determined by the finite element analysis, and is shown in Figure 1. The average volume fraction of the GFRP plate was approximately  $V_f=44\%$ .

Table 1: Material properties of GFRP constituents.

	Fiber reinforcement	Resin matrix
Material	NCR-glass	Vinylester
Stiffness $E$ (GPa)	72.5	3.40
Density $\rho$ (g/cm <sup>3</sup> )	2.54	1.10
Coefficient of thermal expansion $\alpha$ (K <sup>-1</sup> )	$5.5 \times 10^{-5}$	$6.1 \times 10^{-5}$

### 2.2 Static tensile test

The static tensile tests of woven GFRP were conducted in air, in deionized water, and in one molar hydrochloric acid at 40°C in order to evaluate

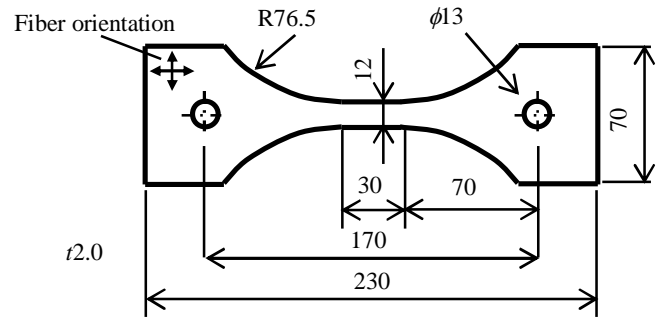


Figure 1: Specimen geometry for tensile test.

its mechanical properties and to determine the stress levels of the constant tensile load tests in each experimental condition. The tensile loading was introduced by means of a 250-kN capacity testing machine. The testing speed was 0.5mm/min, and a strain gauge was bonded in the gauge section of the specimen to measure the axial strain during the test. The tests in both solutions, deionized water and hydrochloric acid, were conducted by attaching a vinyl bag and a silicon plug to the specimen, and filling the vinyl bag with each solution. The experimental setup for static tensile tests is shown in Figure 2.



Figure 2: Experimental setup for static tensile tests in deionized water and hydrochloric acid.

### 2.3 Constant tensile load test

The constant tensile load tests of woven GFRP were conducted in air, in deionized water, and in one molar hydrochloric acid at 40°C in order to evaluate the strain history and the fracture time. The constant tensile load tests were conducted using a creep testing machine. The tests in corrosive solutions; deionized water and hydrochloric acid, were conducted by attaching a vinyl bag which is filled

with each solution to the specimen. A strain gauge was bonded in the gauge section of the specimen to measure the axial strain on the specimen during the test. The experimental setup is shown in Figure 3.



Figure 3: Experimental setup for constant tensile load tests in deionized water and hydrochloric acid.

### 3 Lifetime prediction

The fracture time of GFRP under constant tensile load in deionized water and in hydrochloric acid was predicted based on the assumption of the global load sharing (GLS). This assumption is widely used in the strength calculation of the unidirectional composites which possess low fiber/matrix interfacial adhesion, for example C/C composites. Due to the weak fiber/matrix interfacial adhesion, the stress concentration in the vicinity of the broken fiber and the adjacent fibers is ignored in the strength calculation. It is obvious that the fiber/matrix interfacial adhesion of GFRP after immersion in deionized water and in hydrochloric acid decreases and leads to the assumption of the GLS. In fact, residual strength of unidirectional GFRP after hydrothermal aging, i.e. immersion in deionized water, was calculated by the assumption of GLS and showed a good agreement with the experimental data by considering the degradation of its constituents [9]. Besides, it is reported in previous researches that the fracture of woven GFRP are dominant to the fracture of the glass fiber aligned toward the loading direction, so we also assumed that the strength of the woven GFRP  $\sigma_{\text{GFRP}}$  would be proportional to the strength of the unidirectional GFRP  $\sigma_{\text{UNI}}$  whose fiber is aligned toward the

loading direction. The relationship between both strengths is shown in the following equation:

$$\sigma_{\text{GFRP}} = \alpha \sigma_{\text{UNI}} \quad (1)$$

The strength of the unidirectional GFRP will be calculated using the representative volume element (RVE) in present paper [9]. The RVE discussed in the present paper considers the effect of the interfacial debonding length, which is shown in Figure 4.

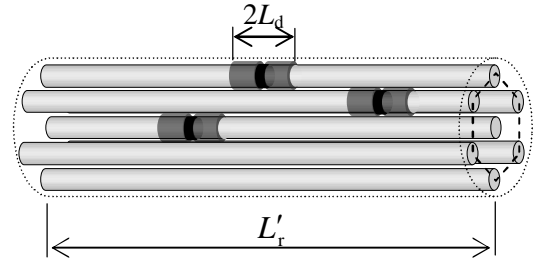


Figure 4: Representative volume element (RVE) of unidirectional GFRP.

First, the average fiber stress  $\sigma_{\text{ave}}^f$  is expressed by the stress of the broken fiber  $\sigma_0^f$  and the unbroken fiber  $\sigma_b^f$  using the cumulative probability of fiber failure  $P(\sigma)$  as following equation:

$$\begin{aligned} \sigma_{\text{ave}}^f &= \sigma_0^f [1 - P(\sigma_0^f)] + \sigma_b^f P(\sigma_0^f) \\ \therefore P(\sigma^f) &= 1 - \exp\left[-\frac{L'_r}{L_0} \left(\frac{\sigma^f}{\sigma_0}\right)^m\right] \end{aligned} \quad (2)$$

where  $L'_r$  is the stress recovery length,  $L_0$  is the referential length ( $=25\text{mm}$ ),  $\sigma_0$  is the scale parameter and  $m$  is the shape parameter. The stress recovery length  $L'_r$  considers the effect of the interfacial debonding length  $L_d$ . The effective length considering is expressed in the following equation [10]:

$$L'_r = L_r + L_d \quad (3)$$

The interfacial debonding length is expressed in following equation [11]-[12]:

$$L_d = -\frac{1}{\alpha} \ln \left[ 1 - \frac{H_2}{H_1} \left( \sigma_0^f + \sigma_{z,\text{swell}}^m - \frac{4\tau^i}{\beta d^f} \right) \right] \quad (4)$$

where  $\alpha$ ,  $\beta$  and  $H_2$  are constants,  $H_1$  is the function of the fiber stress in the longitudinal direction,  $\sigma_{z,\text{swell}}^m$  is the swelling stress of the matrix resin in the longitudinal direction induced by water absorption,  $\tau^i$  is fiber/matrix interfacial shear stress and  $d^f$  is the fiber diameter.  $H_1$  and  $H_2$  are:

$$H_1 = \frac{\mu v^m E^m (\sigma_0^f + \sigma_{z,swell}^m)}{(1-v^f)E^m + (1+v^m)E^f} \quad (5)$$

$$H_2 = \frac{\mu v^f E^m E^f}{(1-v^f)E^m + (1+v^m)E^f}$$

where  $\mu$  is the coefficient of friction.

Finally, the strength of the GFRP  $\sigma_{GFRP}$  will be calculated using the rule of mixture as follows:

$$\sigma_{GFRP} = \alpha \sigma_{UNI} = \alpha (\sigma_{ave}^f V_{FUNI} + \sigma_m (1 - V_{FUNI})) \quad (6)$$

where  $V_{FUNI}$  is the fiber volume fraction of the composite in the loading direction ( $V_{FUNI} = V_f/2 = 22\%$ ). In the lifetime prediction, the strength degradation of the glass fiber ( $\sigma_0$  and  $m$ ) and the fiber/matrix interfacial adhesion ( $\tau_i$ ) were substituted into the calculation to consider the degradation during the constant tensile load tests.

## 4 Results and Discussions

### 4.1 Mechanical properties of woven GFRP

The stress-strain curves obtained from the static tensile tests at various conditions are shown in Figure 5. It is described in the figure that the stress-strain curve shows a viscoelastic response. This is due to the mechanical properties of the matrix resin because that the GFRP has relatively small volume fraction toward the loading direction. It is also shown in the figure that the mechanical properties of woven GFRP decrease in the deionized water and in hydrochloric acid. The mechanical properties of woven GFRP in various environments are listed in table 2. The ultimate tensile strength  $\sigma_{UTS}$  and the rupture strain decrease 10.3% and 16.2% respectively in spite of with its high corrosion resistance. These decreases in the mechanical properties are induced by the damage accumulation which is generated by the solutions. Besides, the experimental condition, i.e. the stress level, of the

Table 2: Mechanical properties of GFRP in various environments

Environment	Tensile strength $\sigma_{UTS}$ (MPa)	Rupture strain $\varepsilon_f$ (%)	Stiffness $E$ (GPa)
Air	339	1.79	24.4
Deionized water	320	1.68	23.5
HCl (1.0mol/l)	304	1.50	24.5

constant tensile load test was determined from the results of the static tensile tests.

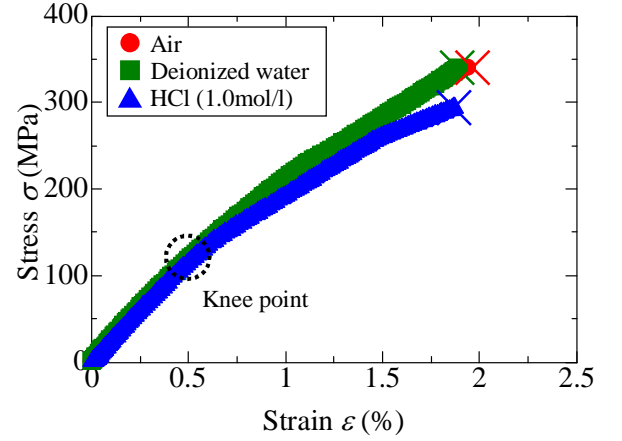


Figure 5: Stress-strain curves of woven GFRP in various environments.

### 4.2 Delayed fracture of GFRP in corrosive environment

The strain curve obtained from the constant tensile load tests in various solutions is shown in Figure 6. It is depicted in the figure that the strain is higher in the order of air, deionized water, and hydrochloric acid. It is suggested that such difference is induced by the decrease in the stiffness due to the immersion into each solution which can be ascertained in the results of the static tensile tests. Fracture occurred in deionized water and in hydrochloric acid but did not occur in air. In addition, rupture strain of the constant tensile load tests were lower than those

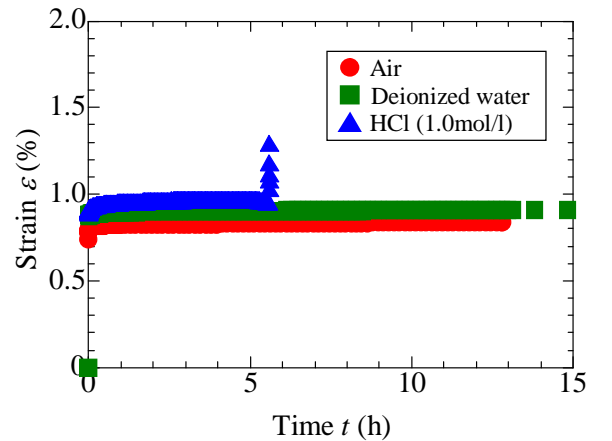


Figure 6: Strain behavior of woven GFRP in various environments ( $\sigma_{app}/\sigma_{UTS}=0.60$ ).

## DAMAGE ACCUMULATION AND LIFETIME PREDICTION OF WOVEN GFRP UNDER CONSTANT TENSILE LOAD TEST IN HYDROCHLORIC ACID SOLUTION

obtained from the static tensile tests. It is obvious that the strength of the woven GFRP is decreasing during the tests in both solutions. The relationship between the applied stress and the fracture time is shown in Figure 7. The fracture time in hydrochloric acid is shorter than that in deionized water. In addition, the fracture time lengthens with the decrease in the applied stress and shows the possibility of the existence of the threshold stress of fracture.

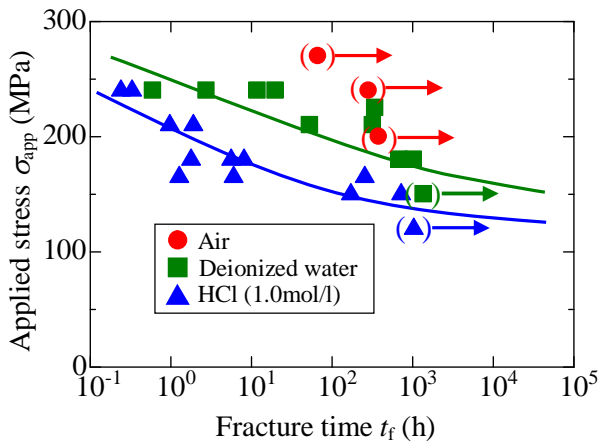


Figure 7: Relationship between the applied stress and fracture time obtained from constant tensile load test in various environments.

The fracture surfaces of woven GFRP after constant tensile load tests were observed using scanning electron microscope (SEM). The fracture surface of woven GFRP in deionized water is shown in Figure 8 and in hydrochloric acid is shown in Figure 9. The SEM pictures in low magnification show the surface of the glass fiber which is aligned in the transverse direction and pictures in high magnification shows the fracture surface of the glass fiber in the loading direction, respectively. It is obvious in the fracture surfaces that the resin adhesion on the fiber surface decreases with the increase in the test time. This transition in the fiber surface shows the decrease of the fiber/matrix interfacial adhesion. It is also ascertained in the fracture surfaces of the glass fiber flatten with the decrease of the applied stress. It is reported in previous researches that the glass fiber strength is dominated by the surface flaw which is built up while manufacturing the glass fiber and the surface flaw propagates by the stress corrosion generated by the applied stress and the solution. Thus the fracture surface of the glass fiber flattens as

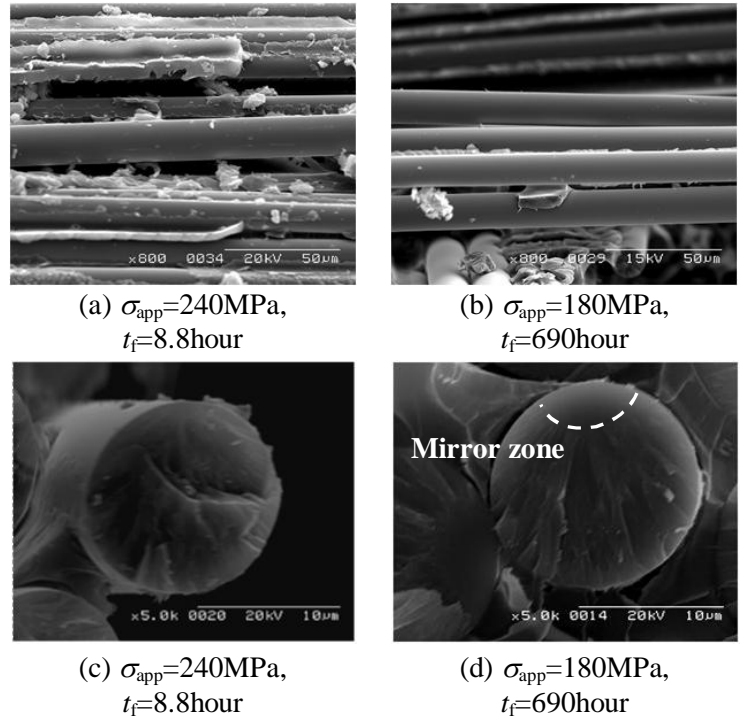


Figure 8: Fracture surface of woven GFRP in deionized water.

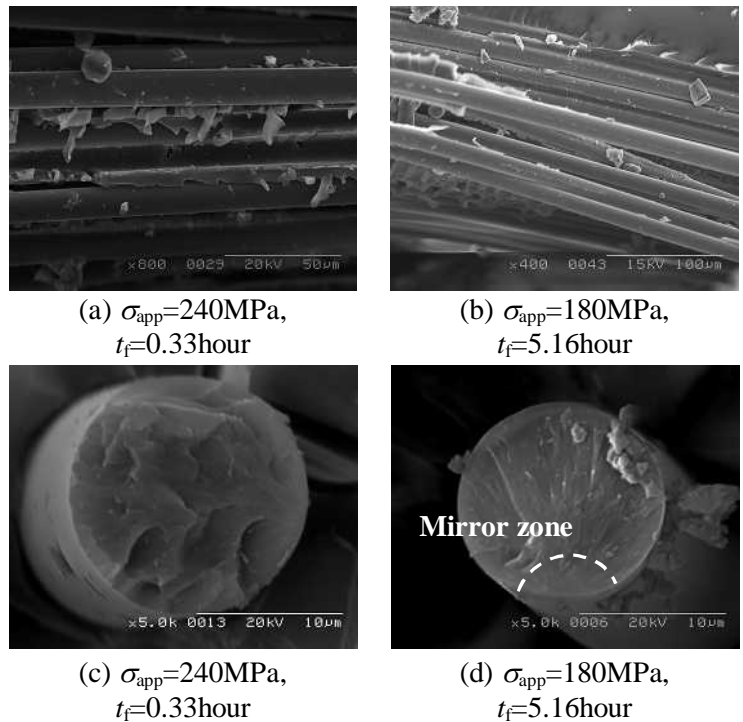


Figure 9: Fracture surface of woven GFRP in hydrochloric acid.

the surface flaw propagates. The delayed fracture of GFRP occurs when the strength of GFRP decreases

and reaches the applied stress. In addition, the applied stress on the GFRP is mainly held by the glass fiber aligned toward the loading direction. Thereafter, the fracture surface of the glass fiber in equal applied stress in deionized water and in hydrochloric acid possess the similar flatness. From these transitions in the fracture surfaces of GFRP, the decrease of the fiber/matrix interfacial adhesion and the glass fiber strength were ascertained.

### 4.3 Lifetime prediction based on GLS

The lifetime of woven GFRP under constant tensile load were predicted based on GLS and the predicted results are shown in Figure 10. The fiber strength ( $\sigma_0$  and  $m$ ) and the fiber/matrix interfacial shear stress ( $\tau$ ) used in the lifetime prediction were obtained from the fiber fragmentation tests of the single fiber composite. The strength degradation of the glass fiber was predicted using the subcritical crack growth model by evaluating the strain history of the constant tensile load test [13]. The degradation of the interfacial shear stress was evaluated by the elastic analysis considering the interfacial debonding length. The predicted results showed good agreement with the experimental data and expresses the validity of the lifetime prediction method proposed in the present paper.

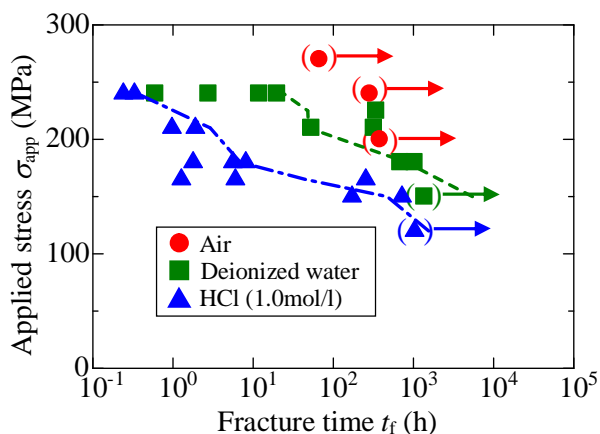


Figure 10: Lifetime prediction based on the GLS assumption.

### Conclusion

In order to clarify the damage accumulation of the corrosion resistant GFRP corrosive environment, the constant tensile load test in air, in deionized water and in hydrochloric acid was conducted. The strain

of woven GFRP under constant tensile load increased in the order of tests in air, deionized water and hydrochloric acid. Besides, the delayed fracture occurred in deionized water and in hydrochloric acid but did not occur in air. The fracture time was shorter in the hydrochloric acid than in deionized water. The decrease of the resin adhesion with the increase of the test time was confirmed, which certifies the degradation of the fiber/matrix resin adhesion. The fracture time was predicted by the assumptions of the global load sharing (GLS). The strength degradation of the glass fiber and the fiber/matrix interfacial adhesion were substituted into the strength calculation of woven GFRP. The good agreement with the predicted results and the experimental data was obtained in both solutions.

### Acknowledgment

This work was supported by Mizuho Foundation for the Promotion of Sciences.

### References

- [1] Y. Fujii, *Journal of the Society of Materials Science* Vol. 54, No. 1, pp.112-113, 2005.
- [2] B. A. Magid, S. Ziaee, K. Gass, M. Schneider, *Composite Structures* Vol. 71, pp.320-326, (2005).
- [3] J. N. Price and D. Hull, *Composites Science and Technology* Vol. 28, pp.193-210, (1987).
- [4] S. N. Saplidis, P. J. Hogg, and S. J. Youd, *Journal of Materials Science* Vol. 32, pp.309-316, (1997).
- [5] M. Kotani, Y. Yasufuku, Y. Tamaishi, and H. Kawada, *JSME International Journal* Vol. 4, No. 11, pp. 1574-1584, (2010).
- [6] F. R. Jones, J. W. Rock, and J. E. Bailey, *Journal of Materials Science*, Vol. 18, pp.1059-1071, 1983.
- [7] M. Kotani, Y. Yasufuku, N. Inoue, K. Kurihara and H. Kawada, *DURACORSYS 2010*, in CD-ROM, (2010)
- [8] A. Turon, J. Costa, P. Maimi, D. Trias and J. A. Mayugo, *Composites Science and Technology* Vol. 65, pp.2039-2048, (2005).
- [9] M. Kotani, Y. Shibata and H. Kawada, *Proceedings of ICCM-17*, (2009).
- [10] A. B. Morais, *Composites Science and Technology* Vol. 61, 1571-1580 (2001).
- [11] A. B. Morais, *Composites Science and Technology* Vol. 66, 2990-2996 (2006).
- [12] K. Liao and Y.M. Tan, *Composites: Part B* Vol. 32, 365-370 (2001).
- [13] M. Kotani and H. Kawada, *ACCM-6*, pp.135-138, (2008).